

On the Sensitivity of SMT Systems to Oscillator Phase Noise over Doubly-Selective Channels

Aamir Ishaque and Gerd Ascheid

*Institute for Communication Technologies and Embedded Systems, RWTH Aachen University, Germany

Email: {ishaque,ascheid}@ice.rwth-aachen.de

Abstract—In this paper, we analyze the effects of oscillator phase noise and doubly-selective fading channel on the performance of the staggered multitone (SMT) system. Unlike the more familiar discrete multitone (DMT) systems, SMT is shown to be insensitive to self-interference effects due to phase noise. The impeding channel and phase noise interference coefficients are defined and theoretical expressions for the inter-carrier and inter-symbol interference are derived to establish solid analytical basis. We demonstrate the resilience of SMT waveform to phase noise distortion and channel fading effects in numerical experiments using appropriate models and the theoretical considerations are shown to fit well with simulation findings. Our assessment indicates that SMT system performs nearly as well as the classical DMT modulation for non-dispersive channels, while it outperforms DMT system by 2 dB for the studied fading channel scenario and fixed equalization complexity for both systems.

Keywords: Phase noise, Fading channels, SMT systems, Prototype filters, SER, SINR.

I. INTRODUCTION

Staggered multitone (SMT) is a promising waveform candidate for beyond 4G systems due to its robustness to Doppler spread and high spectral efficiency [1], relative to discrete multitone (DMT) deployed in many communications systems of the time, e.g., LTE, WiMAX, wireless LAN and DVB. A generalized version of DMT called filtered multitone (FMT) has been considered in wired systems (e.g., in VDSL [2]) and future wireless communication systems for controlling out-of-band leakage [3]. In the same way as the contemporary DMT and FMT systems, being a multicarrier waveform, SMT is also sensitive to random phase fluctuations between transmitter and receiver frequency synthesizers, commonly designated as oscillator phase noise. It is well-known that when prototype filters at the transmitter and receiver maintain subcarrier orthogonality while at the same time satisfying Nyquist ISI-free criterion, there is neither *real-valued* inter-carrier (ICI) nor inter-symbol (ISI) interference components under ideal conditions. But a complex web of interference appears to cause power leakage among data symbols as the perfect reconstructability is compromised at the receiver by amplitude and phase distortions. Their unique characteristics in SMT waveforms depend on the channel and synchronization conditions: 1) Inability of the oscillator to generate a pure carrier signal introduces time-varying phase distortions and hence both ICI and ISI, 2) ICI is caused by the frequency-selective channels due to intrinsic contamination, and 3) Time variation of channel destroys subcarrier orthogonality but more notably introduce ISI.

The effects of phase noise on DMT and FMT systems have been studied in [3]–[5] that showed the relation of phase noise

spectrum to FMT performance and its reduced susceptibility to self-interference. Authors concluded in [6] that the difference in ICI levels between FMT and DMT is rather small and both systems have similar performance for coherent receivers. In [7], authors discuss the tolerable phase noise levels in DMT, when a common phase error (CPE) correction method is used. It was concluded that SER can be improved when 3-dB linewidth (of the low-pass filter used for phase noise synthesis) is of the order of subcarrier spacing or otherwise ICI is dominant and compensation is interference limited. In [8], a filter optimization technique was employed to enhance the robustness against carrier-frequency-offset (CFO). However, it was revealed that conventional prototype filters were inherently immune to CFO effects and optimization gain was at max around 2–3 dB. A multitap equalization solution was proposed in [9] to combat non-flat frequency response in each subcarrier and inherent intrinsic interference issues in SMT systems.

Contribution: The objective of this paper is to analyze the performance of SMT modulation in the presence of phase noise and propagation channel time-frequency selectivity. Through our in depth analysis, we derive expressions for interference components that depict loss of orthogonality and dependence on channel and phase noise defining metrics. Numerical results validate our analytical findings and a comparison against DMT system is presented under similar channel conditions and equalizer design. To the best of our knowledge, not much is known about SMT's behavior in the presence of oscillator phase noise, let alone the channel dispersion. To gain more insight into phase noise characterization for SMT systems, we will nevertheless resort to non-fading scenario.

Notation: $(\cdot)^*$ denotes complex conjugation operation while \otimes represent convolution; $\mathcal{E}\{\cdot\}$, $\Re\{\cdot\}$ and $\Im\{\cdot\}$ refer to expectation, real and imaginary operators respectively; $j^2 = -1$; \mathcal{R} (\mathcal{C}) denote real (complex) numbers while $\mathcal{CN}(\mu, \sigma^2)$ is a complex proper Gaussian distribution with mean μ and variance σ^2 .

II. SMT MODULATION SYSTEM

Figure 1 illustrates the block diagram of an SMT transceiver that transmits real-valued data symbols $a_{m,k}$ obtained from M_Q -QAM constellation using complex-to-real transformation and then filtered by a symmetric real-valued prototype filter $p(n)$ after IFFT operation. The transmit signal is collected into a sequence of discrete-time signal $x(n)$ as:

$$x(n) = \sum_{m=-\infty}^{+\infty} \sum_{k=0}^{K-1} p(n - mM) e^{j\frac{2\pi}{K}kn} e^{j\varphi_{m,k}} a_{m,k} \quad (1)$$

where the pre-processing coefficients are usually selected as $\varphi_{m,k} = (m+k)\pi/2 - mk\pi$ [10]. It should be noted that the synthesis $p(n)$ and analysis $q(n)$ filter-pairs can be efficiently incorporated with K -sized FFT and IFFT by employing polyphase filtering structures [11]. Consider a time-variant

*Part of this work has been performed in the framework of the FP7 project ICT-317669 METIS, which is partly funded by the European Union. The authors would like to acknowledge the contributions of their colleagues in METIS, although the views expressed are those of the authors and do not necessarily represent the project.

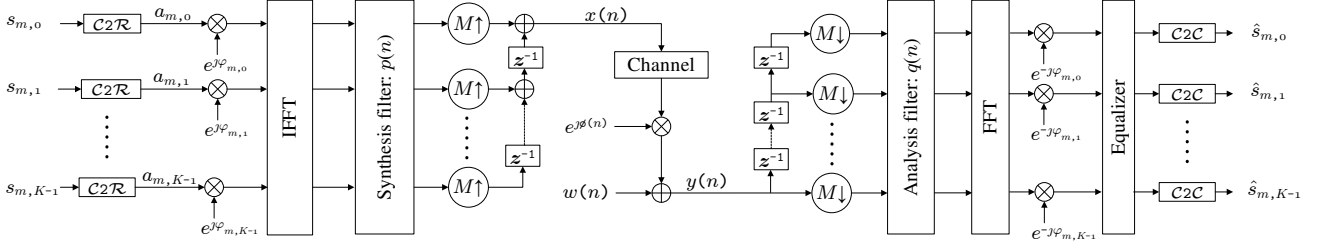


Fig. 1. A generic baseband SMT system in the presence of phase noise and time-variant fading channel.

multipath channel $h_l(n)$ and a phase noise process $\phi(n)$, then the received signal can be written as follows:

$$y(n) = e^{j\phi(n)} \sum_{l=0}^{L-1} x(n-l)h_l(n) + w(n) \quad (2)$$

where $w(n) \sim \mathcal{CN}(0, \sigma_w^2)$ are circularly-symmetric additive noise samples. After the analysis filterbank, we can express the output at m' -th symbol and k' -th subcarrier as:

$$z_{m',k'} = e^{-j\varphi_{m',k'}} \sum_{n=-\infty}^{+\infty} q(n-m'M) e^{-j\frac{2\pi}{K}k'n} y(n) \quad (3)$$

$$\begin{aligned} &= \mathcal{I}_{m',k'}^{m',k'} a_{m',k'} + \sum_{\substack{m=-\infty \\ m \neq m'}}^{+\infty} \mathcal{I}_{m,k'}^{m',k'} a_{m,k'} \\ &+ \sum_{m=-\infty}^{+\infty} \sum_{\substack{k=0 \\ k \neq k'}}^{K-1} \mathcal{I}_{m,k}^{m',k'} a_{m,k} + \bar{w}_{m',k'} \end{aligned} \quad (4)$$

which shows that the received signal is composed of the true symbol multiplied by $\mathcal{I}_{m',k'}^{m',k'}$ and a weighted sum of contributions from other symbols and subcarriers. For an ideal system, correlation between the transmit and receive filters is represented by the ambiguity function: $A_{m,k}$. The interference components in (4) with mapping $(m, k) \rightarrow (m', k')$ are defined as:

$$\begin{aligned} \mathcal{I}_{m',k'}^{m',k'} &= \sum_{n=-\infty}^{+\infty} \sum_{l=0}^{L-1} q(n-m'M) p(n-l-mM) \\ &\times h_l(n) e^{j\phi(n)} e^{j\frac{2\pi}{K}((k-k')n-kl)} e^{j(\varphi_{m,k}-\varphi_{m',k'})} \end{aligned} \quad (5)$$

$$\begin{aligned} &\approx \sum_{n=-\infty}^{+\infty} g_{m',m}(n) H_k(n) e^{j\phi(n)} \\ &\times e^{j\frac{2\pi}{K}(k-k')n} e^{j(\varphi_{m,k}-\varphi_{m',k'})} \end{aligned} \quad (6)$$

where $g_{m',m}(n) = q(n-m'M)p(n-mM)$, (6) is a reasonable approximation, if the channel frequency-selectivity is mild, so that $\sum_{l=0}^{L-1} p(n-l-mM)h_l(n)e^{-j\frac{2\pi}{K}kl} \approx p(n-mM)H_k(n)$, and $H_k(n)$ is the channel frequency response (CFR) at the n -th time instant and k -th subcarrier.¹

We assume a wide sense stationary channel process $h_l(n)$ with an uncorrelated scattering environment. The length- L impulse response $h_l(n)$ is modeled by zero-mean independent complex Gaussian random variable (RV). They have exponen-

tial power delay profile:

$$\mathcal{E}_h \{ |h_l(n)|^2 \} = \alpha e^{-\beta l}, \text{ with } \alpha = \frac{1 - \exp(-\beta)}{1 - \exp(-\beta L)} \quad (11)$$

and $\tau_{rms} = 1/\beta$ as the normalized r.m.s delay spread which relates to coherence bandwidth as $B_c \approx 1/(\tau_{rms}T_s)$ [12]. Since the channel is time-variant, the fading coefficients are correlated at times $n'T_s$ and $n''T_s$ represented by:

$$R_{l,q}(n', n'') = \mathcal{E}_h \{ h_l(n')h_q^*(n'') \} \quad (12)$$

$$= \alpha e^{-\beta l} J_0(2\pi f_d |n' - n''|T_s) \delta_{l,q} \quad (13)$$

where f_d is the maximum Doppler shift, $J_0(\cdot)$ is the zero-order Bessel function of the first kind, $\delta_{l,q}$ is the Kronecker delta function and T_s is the sampling duration. Using (11) and (13), the auto-correlation between the frequency coefficients separated by n samples and k subcarriers is given by:

$$\rho_{n,k} = \mathcal{E}_h \{ H_k(n)H_0^*(0) \} \quad (14)$$

$$= \alpha J_0(2\pi f_d n T_s) \sum_{l=0}^{L-1} e^{-\beta l} e^{-j\frac{2\pi}{K}lk}. \quad (15)$$

If $g_m(n) = q(n)p(n-mM)$ and $\bar{H}_{m,k} = e^{j\varphi_{m,k}} \sum_{n=-\infty}^{+\infty} g_m(n)H_k(n)e^{j\frac{2\pi}{K}kn}$ is the cross CFR without phase noise, then it can be shown that:

$$\bar{\rho}_{m,k} = \mathcal{E}_h \{ \bar{H}_{m,k}\bar{H}_{0,0}^* \} \quad (16)$$

$$= e^{j\varphi_{m,k}} \sum_{n',n''=-\infty}^{+\infty} g_m(n')g_0(n'')\rho_{n''-n',k} e^{j\frac{2\pi}{K}kn'} \quad (17)$$

and the power of (m, k) -th CFR is $|\bar{A}_{m,k}|^2 = \mathcal{E}_h \{ |\bar{H}_{m,k}|^2 \} = \sum_{n',n''} g_m(n')g_m(n'')\rho_{n''-n',0} e^{j\frac{2\pi}{K}k(n'-n'')}$.

Note that if $f_d = 0$, then $|\bar{A}_{m,k}|^2 = |A_{m,k}|^2$.

The zero-mean stationary phase noise realization $\phi(n)$ resembles practical oscillators in terms of its power spectral density (PSD) shape. One of PSD shape of choice is the so-called *Linear decay* spectrum [13]. The frequency-characterization of the phase noise process is then given by the double-sided PSD as:

$$\mathcal{L}_\phi(f) = 10^{-c} + \begin{cases} 10^{-a} & |f| \leq f_l \\ 10^{-b\frac{f-f_l}{f_h-f_l}-a} & f > f_l \\ 10^{b\frac{f+f_l}{f_h-f_l}-a} & f < -f_l \end{cases} \quad (18)$$

where f_l is 3-dB bandwidth of the reference signal phase noise, the parameters a and c denote noise floors at frequencies lower than f_l and higher than f_h respectively, whereas b represents spectral decay in between the two white noise regions. The inverse Fourier transform of $\mathcal{L}_\phi(f)$ gives the auto-correlation

¹This assumption holds true when subcarrier spacing $f_{sub} = B/K$ is much smaller than coherence bandwidth B_c or prototype filters are sufficiently time-localized. Nonetheless, it is well-known that the benefits of SMT w.r.t DMT lie in high mobility scenarios [1].

$$\mathcal{I}_{m,k}^c = \underbrace{(\bar{\rho}_{m,k} - A_{m,k}) \bar{H}_{0,0} + \sqrt{|\bar{A}_{m,k}|^2 - |\bar{\rho}_{m,k}|^2} \Delta_{m,k}}_{\triangleq T_{m,k}} + j \underbrace{\left(e^{j\varphi_{m,k}} \sum_{n=-\infty}^{\infty} g_m(n) H_k(n) \phi(n) e^{j\frac{2\pi}{K}kn} \right)}_{\triangleq U_{m,k}} \quad (7)$$

$$\begin{aligned} \zeta_{m,k}^{(1)} &= \Re^2 \left\{ \bar{\rho}_{m,k} - A_{m,k} \right\} \mathcal{E}_h \left\{ \left| \Re \left\{ H_{0,0} \right\} \right|^2 \right\} + \Im^2 \left\{ \bar{\rho}_{m,k} - A_{m,k} \right\} \mathcal{E}_h \left\{ \left| \Im \left\{ H_{0,0} \right\} \right|^2 \right\} + \left(|\bar{A}_{m,k}|^2 - |\bar{\rho}_{m,k}|^2 \right) \mathcal{E}_\Delta \left\{ \left| \Re \left\{ \Delta_{m,k} \right\} \right|^2 \right\} \\ &\stackrel{(a)}{=} \frac{|\bar{A}_{m,k}|^2 + |\bar{A}_{m,k}|^2}{2} - \Re \left\{ \bar{\rho}_{m,k} \right\} \Re \left\{ A_{m,k} \right\} - \Im \left\{ \bar{\rho}_{m,k} \right\} \Im \left\{ A_{m,k} \right\} \end{aligned} \quad (8)$$

$$\begin{aligned} \zeta_{m,k}^{(2)} &= \sum_{n', n''=-\infty}^{\infty} g_m(n') g_m(n'') \mathcal{E}_{\phi,h} \left\{ \phi(n') \phi(n'') \left(\Re \left\{ H_k(n') \right\} \Re \left\{ H_k(n'') \right\} \sin \Phi_{m,k}^{(n')} \sin \Phi_{m,k}^{(n'')} + \Im \left\{ H_k(n') \right\} \Im \left\{ H_k(n'') \right\} \right. \right. \\ &\quad \left. \left. \times \cos \Phi_{m,k}^{(n')} \cos \Phi_{m,k}^{(n'')} + \Re \left\{ H_k(n') \right\} \Im \left\{ H_k(n'') \right\} \sin \Phi_{m,k}^{(n')} \cos \Phi_{m,k}^{(n'')} + \Im \left\{ H_k(n') \right\} \Re \left\{ H_k(n'') \right\} \cos \Phi_{m,k}^{(n')} \sin \Phi_{m,k}^{(n'')} \right) \right\} \end{aligned} \quad (9)$$

$$\stackrel{(b)}{=} \sum_{n=-\infty}^{\infty} \sum_{q=-\infty}^{\infty} g_m(n) g_m(n+q) R_\phi(q) R_H^{(\Re)}(q, k) \cos \left(\frac{2\pi}{K} kq \right) \quad (10)$$

function $R_\phi(n) = \mathcal{E}_\phi \{ \phi(m) \phi(m+n) \}$ that is only a function of time difference nT_s . When the variance of the phase samples: $\sigma_\phi^2 = R_\phi(0)$ is small, as is usually the case with realistic frequency synthesizers, the complex exponential can be well captured by the first-order power series approximate:

$$\theta(n) = e^{j\phi(n)} = \sum_{i=0}^{\infty} \frac{(j\phi(n))^i}{i!} \approx 1 + j\phi(n) \quad (19)$$

and similarly, the PSD of $\theta(n)$ is given by: $\mathcal{L}_\theta(f) \approx \delta(f) + \mathcal{L}_\phi(f)$.

III. PROPERTIES OF INTERFERENCE COMPONENTS

Assume the transmission over wide-sense stationary environment (i.e., both the channel and phase noise processes have fixed distributions) and the prototype filters have even symmetry, then interference power computation is independent of the time/frequency points (m', k') . Hence, we omit symbol/subcarrier indices for brevity and treat $\mathcal{I}_{m,k}^{0,0} \triangleq \mathcal{I}_{m,k}$ as a general interference component originating from k -th subcarrier in m -th symbol.

A. Coherent Receiver

In order to quantify the combined effects of both the channel and phase noise, we derive interference power as a function of correlation functions $\bar{\rho}_{n,k}$ and $R_\phi(n)$ respectively. Since, we have apriori knowledge of channel but an unknown phase process, we adopt the following mean-square-error (MSE) function:

$$\text{MSE} = \mathcal{E} \left\{ \left| \Re \left\{ z_{0,0} - \bar{H}_{0,0} \sum_{m=-\infty}^{+\infty} \sum_{k=0}^{K-1} A_{m,k} a_{m,k} \right\} \right|^2 \right\}. \quad (20)$$

In the sequel, we assume that the channel coefficients $\bar{H}(m, k)$ could be modeled by a correlation model:

$$\bar{H}_{m,k} = \bar{\rho}_{m,k} \bar{H}_{0,0} + \sqrt{|\bar{A}_{m,k}|^2 - |\bar{\rho}_{m,k}|^2} \Delta_{m,k} \quad (21)$$

with $\bar{H}_{0,0}, \Delta_{m,k} \sim \mathcal{CN}(0, 1)$. Now, we can re-define *effective interference* for coherent case from (20) given as (7) at the top of this page.

Remark 1: Given the independence between $\bar{H}_{m,k}, \Delta_{m,k}, \phi(n)$ and $a_{m,k}$, it is obvious that each interference term

$\zeta_{m,k} = \mathcal{I}_{m,k}^c a_{m,k}$ is statistically-independent, zero-mean and has variance $\mathcal{E}_{h,\phi} \left\{ \left| \Re \left\{ \zeta_{m,k} \right\} \right|^2 \right\} = \zeta_{m,k} \sigma_a^2$. In summary, (20) can be simplified as: $\text{MSE} = \sigma_w^2/2 + \sigma_a^2 \sum_{m,k} \zeta_{m,k}$.

Remark 2: For the sake of exposition, assume a phase-noise-free system, then the second term in (20) is the expected intrinsic response for a single-tap equalizer. In essence, closer the expected response is to a noiseless observation, better orthogonalized SMT design is. This implies that SMT system should be designed such that $\Re \left\{ \sum_{m,k} \bar{H}_{m,k} a_{m,k} \right\} \simeq \Re \left\{ \bar{H}_{0,0} \sum_{m,k} A_{m,k} a_{m,k} \right\}$ for all channel realizations $h_l(n)$ in the distribution. Knowing that only real part is relevant, a simple zero-forcing equalizer yields the symbol estimates: $\hat{a}_{0,0} = \Re \left\{ z_{0,0} / \bar{H}_{0,0} \right\}$. As a result, $z_{0,0}$ in (4) can be easily seen to retain a correlated component due to limited auto-correlation $0 \leq |\bar{\rho}_{m,k} - A_{m,k}| \leq |A_{m,k}|$ and an uncorrelated term that is aligned with the real field. These components can be linked directly to a processed interference in (7). In a non-time-varying flat fading scenario, $\bar{\rho}_{m,k} = A_{m,k}$ and $T_{m,k} = 0, \forall m, k$.

Remark 3: The perfect knowledge of $\bar{H}_{0,0}$ means that the desired signal is self-affected by the phase noise distortion, since $|\Re \left\{ \mathcal{I}_{0,0}^c \right\}| = |\Im \left\{ U_{0,0} \right\}| \geq 0$, where the equality holds if $H_k(n) = 1, \forall k, n$ (more on this special case in Section III-B).

Given a certain channel $h_l(n)$ and phase noise $\phi(n)$ realization, the effective signal-to-interference-plus-noise ratio (SINR) is defined as:

$$\text{SINR}(h, \phi) = \frac{|\Re \left\{ A_{0,0} \right\}|^2}{\left| \Im \left\{ U_{0,0} \right\} \right|^2 + \underbrace{\sum_{m=-\infty}^{+\infty} \sum_{k=0}^{K-1} \left| \Re \left\{ \mathcal{I}_{m,k}^c \right\} \right|^2}_{(m,k) \neq (0,0)}} + \text{SNR}^{-1} \quad (22)$$

where $\text{SNR} = 2\sigma_a^2/\sigma_w^2$ and $\Re \left\{ A_{0,0} \right\} = 1$ for orthogonal designs. If we approximate interference components $\mathcal{I}_{m,k}^c$ as Gaussian distributed, then for M_P -PAM symbols $a_{m,k}$, the symbol-error-probability (SEP) is well-known as [12]:

$$P_s = 2 \left(1 - \frac{1}{M_P} \right) \mathcal{E}_{h,\phi} \left\{ \mathcal{Q} \left(\sqrt{\frac{3}{M_P^2 - 1} \text{SINR}(h, \phi)} \right) \right\} \quad (23)$$

where $\mathcal{Q}(\cdot)$ is the Gaussian Q-function. In general, the SEP from (23) is not analytically tractable, we hence focus on the power of interference components $\mathcal{I}_{m,k}^c$ instead. Let $\Phi_{m,k}^{(n)} \triangleq \frac{2\pi}{K}kn + \varphi_{m,k}$, then the power of the RVs $\Re\{T_{m,k}\}$ and $\Im\{U_{m,k}\}$ denoted by $\varsigma_{m,k}^{(1)} = \mathcal{E}_h \left\{ |\Re\{T_{m,k}\}|^2 \right\}$ and $\varsigma_{m,k}^{(2)} = \mathcal{E}_h \left\{ |\Im\{U_{m,k}\}|^2 \right\}$ respectively are given at the top of the previous page, where (a) follows from the fact that $\Delta(m,k)$ and $\bar{H}(m,k)$ are uncorrelated, and in step (b) made the substitution $q = n' - n''$ and employed the channel cross-correlation $R_H^{(\Re)}(q,k) = \mathcal{E}_h \left\{ \Re\{H_k(n)\} \Re\{H_k(n+q)\} \right\} = J_0(2\pi q f_d T_s)/2$ and $R_H^{(\Im)}(q,k) = \mathcal{E}_h \left\{ \Im\{H_k(n)\} \Im\{H_k(n+q)\} \right\} = R_H^{(\Re)}(q,k)$, since $h_i(n)$ is a proper RV. Finally, $\varsigma_{m,k} = \varsigma_{m,k}^{(1)} + \varsigma_{m,k}^{(2)}$ gives us the total power of $\mathcal{I}_{m,k}^c$. Several key properties of $\mathcal{I}_{m,k}^c$ can be outlined from (7)-(10) and (17).

- From (8), $\varsigma_{m,k}^{(1)}$ is an indicator of channel dispersion as $\varsigma_{m,k}^{(1)} \rightarrow 0, \forall m,k$ under ideal channel conditions and worsens with higher selectivity. The former can be proved under the limit of slow-flat fading cases by the fact that $\bar{\rho}_{m,k}$ is purely imaginary for $(m,k)_{\text{mod}2} \neq (0,0)$, (i.e. $\Re\{\bar{\rho}_{m,k}\} = \Re\{A_{m,k}\} = 0, \Im\{\bar{\rho}_{m,k}\} = \Im\{A_{m,k}\}$ and $|A_{m,k}|^2 = |\bar{A}_{m,k}|^2$).
- If the channel is frequency-flat over the entire bandwidth B , then defining $\tilde{A}_{m,k}(\nu) = \sum_{n=-\infty}^{+\infty} J_\nu(2\pi f_d T_s n) g_m(n) \exp(j\frac{2\pi}{K}kn)$, we have $\bar{\rho}_{m,k} = e^{j\varphi_{m,k}} \sum_{\nu=-\infty}^{+\infty} \tilde{A}_{m,k}(\nu) \tilde{A}_{0,0}(\nu)$ and $|\bar{A}_{m,k}|^2 = \sum_{\nu=-\infty}^{+\infty} |\tilde{A}_{m,k}(\nu)|^2$. Moreover, for small but realistic Doppler spectrum, $\nu = 0$ gives a reasonable approximate. Thus, $\bar{\rho}_{m,k} \approx J_0(2\pi m M f_d T_s) A_{m,k}$ and $|\bar{A}_{m,k}|^2 \approx |J_0(2\pi m M f_d T_s)|^2 |A_{m,k}|^2$ so that for $(m,k)_{\text{mod}2} \neq (0,0)$:

$$\varsigma_{m,k}^{(1)} = \frac{\left(1 - J_0(2\pi m M f_d T_s)\right)^2}{2} |A_{m,k}|^2 \quad (24)$$

which causes both ISI and ICI but all the distortion arises from $m \neq 0$ symbols as $\varsigma_{0,k}^{(1)} = 0$ for all k .

- For the opposite case of entirely frequency-selective channels, we have $\bar{\rho}_{m,k} = \rho_{0,k} A_{m,k}, |A_{m,k}|^2 = |\bar{A}_{m,k}|^2$ and,
$$\varsigma_{m,k}^{(1)} = \begin{cases} (1 - \Re\{\rho_{0,k}\}) |A_{m,k}|^2, & (m,k)_{\text{mod}2} = (0,0) \\ (1 - \Im\{\rho_{0,k}\}) |A_{m,k}|^2, & (m,k)_{\text{mod}2} \neq (0,0) \end{cases} \quad (25)$$

where a lack of ISI is obvious for all m .

B. AWGN Channel

In this section, we try to gain more insight into the impact of phase noise by neglecting the influence of channel. Then, (6) can be re-written as:

$$\mathcal{I}_{m,k} = \sum_{n=-\infty}^{+\infty} g_m(n) e^{j\phi(n)} e^{j\Phi_{m,k}^{(n)}}. \quad (26)$$

The statistical parameters of CPE's distribution are essential because their significance implies the achievable gain with any

CPE correction method. The mean of $\Re\{\mathcal{I}_{0,0}\}$ is:

$$\mu_{0,0} = e^{-\sigma_\phi^2/2} \sum_{n=-\infty}^{+\infty} g_0(n) = e^{-\sigma_\phi^2/2} \quad (27)$$

and the variance: $\sigma_{0,0}^2 = \mathcal{E}_\phi \left\{ |\Re\{\mathcal{I}_{0,0}\}|^2 \right\} - \mu_{0,0}^2$ of the CPE term can be derived as:

$$\sigma_{0,0}^2 = \frac{e^{-\sigma_\phi^2}}{2} \sum_{n'=-\infty}^{+\infty} \sum_{n''=-\infty}^{+\infty} g_0(n') g_0(n'') \times \left(e^{R_\phi(n'-n'')} + e^{-R_\phi(n'-n'')} \right) - e^{-\sigma_\phi^2} \quad (28)$$

where we used the fact that $\phi(n) \sim \mathcal{N}(0, \sigma_\phi^2)$ and $\mathcal{E}\{e^{j\phi(n)}\} = e^{-\sigma_\phi^2/2}$. It is worth noting that the convergence of $\mu_{0,0}$ to $A_{0,0}$ for negligible phase noise is implicit. Another key aspect is that (27) has the same value as it would have been in DMT and FMT systems [4] but the basic difference lies in (28). In fact, it can be deduced by simply using the approximate phase model (19) giving:

$$\Re\{\mathcal{I}_{m,k}\} \approx \Re\{A_{m,k}\} - \sum_{n=-\infty}^{+\infty} \phi(n) g_m(n) \sin \Phi_{m,k}^{(n)} \quad (29)$$

where interestingly, we note that the block-wise mean of phase process $\phi(n)$ is entirely aligned across imaginary axis² i.e., $\mathcal{I}_{0,0} = A_{0,0}$. It can hence be concluded that CPE correction in SMT system would not be beneficial.

Noting that variance of $\Re\{\mathcal{I}_{m,k}\}$ given by $\sigma_{m,k}^2 = \mathcal{E}_\phi \left\{ |\Re\{\mathcal{I}_{m,k}\}|^2 \right\}$ is due to the random term in (29), a general expression for $\sigma_{m,k}^2$ can be computed as follows:

$$\sigma_{m,k}^2 = \sum_{n=-\infty}^{+\infty} \sum_{q=-\infty}^{+\infty} g_m(n) g_m(n+q) R_\phi(q) \times \sin \Phi_{m,k}^{(n)} \sin \Phi_{m,k}^{(n+q)}. \quad (30)$$

Let $S_G(f; m, k)$ is the discrete-time Fourier transform of $G(q; m, k) = \sum_{n=-\infty}^{+\infty} g_m(n) g_m(n+q) \exp(j\frac{2\pi}{M}kn)$, then after some manipulation, it can be shown that:

$$\sigma_{m,k}^2 = \frac{1}{4} \left[\int_0^1 S_G(f; m, 0) \times \left(S_\phi \left(-f - \frac{k}{K} \right) + S_\phi \left(-f + \frac{k}{K} \right) \right) df - e^{j\pi(m+k)} \int_0^1 S_G(f; m, k) S_\phi \left(-f - \frac{k}{K} \right) df - e^{-j\pi(m+k)} \int_0^1 S_G(f; m, -k) S_\phi \left(-f + \frac{k}{K} \right) df \right] \quad (31)$$

where $S_\phi(f)$ is the discrete phase noise spectrum given by $S_\phi(f) = (1/T_s) \mathcal{L}_\phi(f/T_s)$, $S_G(f; m, k) = S_{PQ}(f - \frac{k}{M}; m) S_{PQ}^*(f; m)$ and $S_{PQ}(f; m) = P(f) e^{-j2\pi m M f} \otimes Q^*(-f)$. To understand this relation, assume we have ideal prototype filters whose frequency-confined response is given by $P(f) = Q(f) = \text{rect}(Kf)$. Then, by computing $S_G(f; m, k)$, we can see that it will be non-zero for $k = 0$ and

²The CPE is, in essence, the scaled instantaneous mean of $\phi(n)$ in DMT systems [7]. In general, analogy holds for entire ISI in SMT systems with some filtering. For orthogonal prototype filters, $\Re\{\mathcal{I}_{m,0}\} \simeq \pm \sum_{n=-\infty}^{+\infty} \phi(n) g_m(n), \forall m_{\text{mod}2} \neq 0$ is approximately the average of $\phi(n)$ in m -th offset symbol and a zero block-wise average means nearly no existence of ISI. Nevertheless, we called $\Re\{\mathcal{I}_{0,0}\}$ as CPE in (27) and (28).

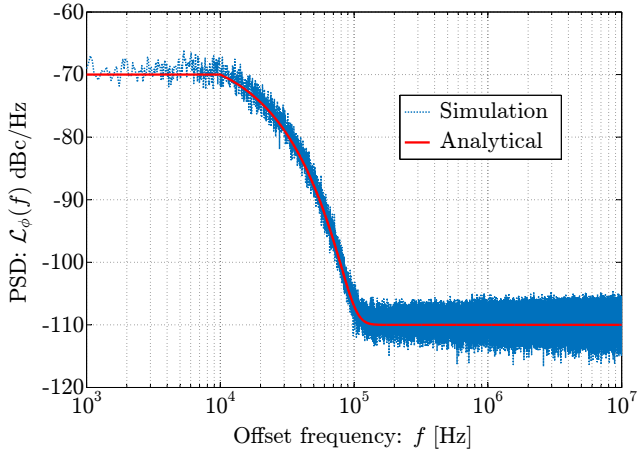


Fig. 2. Power spectral density (single-side) of the phase noise process $\phi(n)$ with $f_l = 10$ KHz.

zero otherwise. From this observation, we can conclude that distortion due to phase noise corresponds to the power of phase noise spectrum inside one subcarrier spacing f_{sub} and ICI arises due to frequency-shifted phase noise PSD: $S_\phi(-f \pm \frac{k}{K})$.

In summary, for a fixed bandwidth B and power of the phase noise spectrum falling inside B , the total interference power is independent of the number of subcarriers K . Increasing the bandwidth B monotonically increases the interference power and, if K is kept constant, then ISI increase might outweigh that in ICI. The PSD of phase noise $S_\phi(f)$ determines the distribution of power amongst various interference components. One can deduce that if $f_h \gg f_{sub}$, ICI has rather minimal effect. For the converse case $f_h \ll f_{sub}$, SMT suffers from relatively lower ICI than DMT due to higher frequency-confinement. It is the combination of prototype filters and PSD of phase noise that defines the robustness against the interfering components. In fact, any realistic prototype filter pair with spectrum $S_G(f; m, k)$ creates side-lobes outside $|f| \geq f_{sub}/2$ and from (31), it has an adverse effect on the phase noise sensitivity.

IV. NUMERICAL ANALYSIS

Simulations are carried out with a multitap channel model with r.m.s delay spread of $\tau_{rms}T_s = 100$ ns (unless otherwise stated differently). The prototype filters $p(n) = q(n)$ are obtained by truncating the sampled version of pulses $p(n) = p(t)|_{t=nT_s}$ from the extended Gaussian function (EGF) [10], to a length $L_{pq} = 4K$ for a system with $K = 128$ subcarriers. We assume the receiver knows perfectly its own channel coefficient but $\bar{H}(m, k)$, $\forall (m, k) \neq (0, 0)$ are unknown. The phase noise process $\phi(n)$ has PSD shape with parameters set to: $f_h = 10f_l$, $a = 7$, $b = 4$, $c = 11$ (shown in Fig. 2) having variance $\sigma_\phi^2 \approx 4 \times 10^{-3}$ at 10 MHz sampling rate and $f_l = 10$ KHz.

In the first set of simulations, we have computed ICI as a function of originating subcarrier location. It shows that ISI in SMT for the most frequency-localized pulse ($\lambda = 1$) is on a par with CPE in DMT and the first subcarrier produced most of the interference. Also, as the localization factor λ gets higher, lesser frequency confinement of the filter caused a shallower ICI fall and decrease in ISI. One can easily conclude that in the absence of phase noise compensator, an ISI resilient pulse ($\lambda \geq 2$) is preferable, whereas if a frequency-domain compensation scheme is employed, the low-pass behavior of SMT ($\lambda \leq 2$) essentially requires lesser-order ICI mitigation.

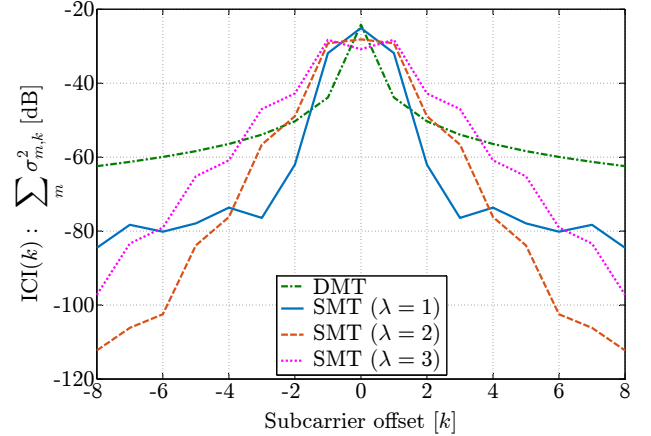


Fig. 3. ICI extension in SMT and DMT systems with AWGN channel, $f_l = 10$ KHz and $B = 10$ MHz. Note that $k = 0$ corresponds to CPE in DMT and ISI in SMT.

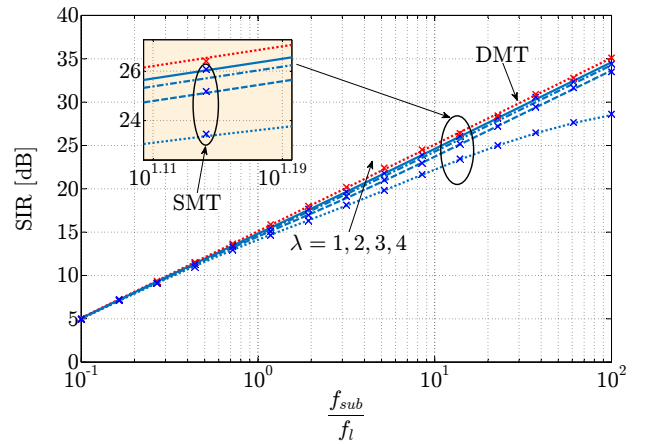


Fig. 4. Signal-to-interference ratio (SIR) versus subcarrier spacing to corner frequency ratio f_{sub}/f_l for a fixed subcarrier number and AWGN channel. Lines and markers indicate analytical and simulation results respectively.

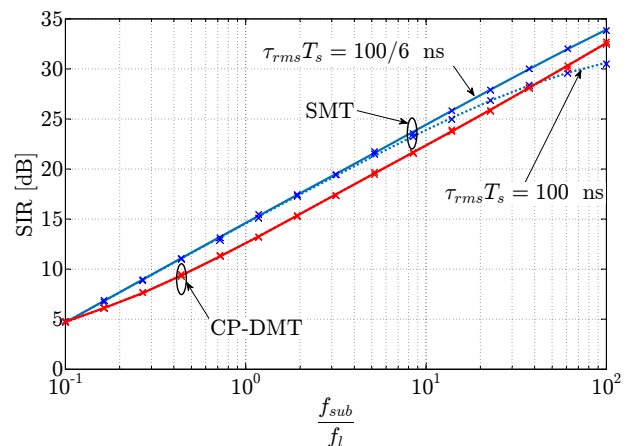


Fig. 5. SIR versus f_{sub}/f_l for a fixed subcarrier number and Rayleigh fading channel with $f_d = 600$ Hz, $L = 3$ and $\lambda = 2$. Lines and markers indicate analytical and simulation results respectively.

In Fig. 4, we study the effect of subcarrier spacing f_{sub} relative to the corner frequency f_l on the SIR performance. A decrease in distortion with f_{sub}/f_l is justifiable because

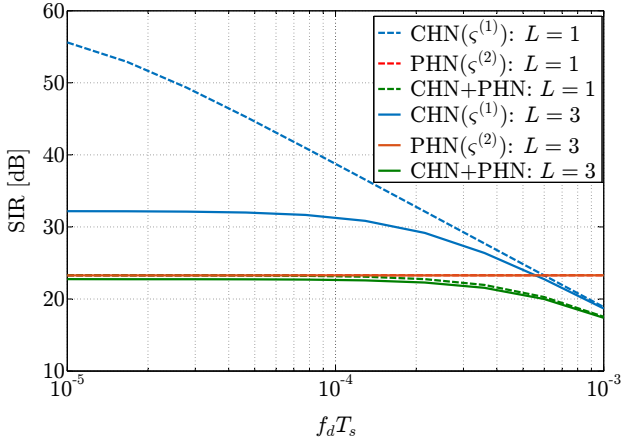


Fig. 6. SIR of SMT system versus normalized Doppler shift $f_d T_s$, $\lambda = 2$ and phase noise with $f_{sub}/f_l \approx 7.8$.

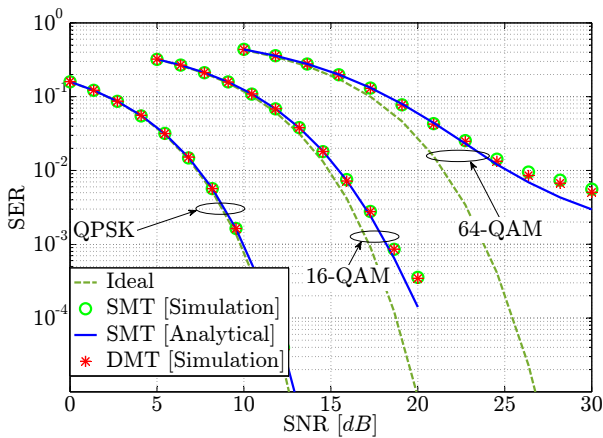


Fig. 7. Symbol error rate (SER) for AWGN channel versus SNR for various constellation sizes with SMT having $\lambda = 2$ and phase noise with $f_{sub}/f_l \approx 7.8$.

smaller f_{sub} relative to f_l will cause ICI components to assemble in the vicinity of the decay region in Fig. 2. Moreover, decreasing f_{sub} will decorrelate phase noise samples. Intuitively, a more *noise-like* phase noise process increases sensitivity to phase noise distortion and as a result, makes the phase noise estimation a challenge. A trade-off in SMT systems is that the reduction of f_{sub} w.r.t B_c reduces the impact of channel frequency-selectivity. It is also shown that the EGF pulse with larger λ outperforms smaller values by reducing ISI contribution (see Fig. 3). In fact, DMT forms an tight upper bound on the SMT performance and is achievable only for larger λ or smaller f_{sub}/f_l . When the transmission suffers from channel fading, we can deduce from Fig. 5 that a gain of up to 2 dB is expected from SMT for the defined channel conditions due to better frequency confinement. The loss in wider spacings can be attributed to SMT's non-orthogonality in frequency-selective channels. The regime $f_{sub} \ll f_l$ is dominated by phase noise and Doppler effects. Due to orthogonality against multipath channel ensured by cyclic-prefix (CP), the interference power in DMT case is independent of channel frequency-selectivity.

We also demonstrate in Fig. 6 the SIR performance of SMT under maximum Doppler shift f_d . As expected, the channel distribution has no influence on the phase noise (PHN) contribution in (10). For the considered phase noise model,

the total SIR performance was overshadowed by phase noise distortion due to a dominant phase noise process. However, an interference breakup shows decreasing SIR of channel (CHN) part in (8) with increasing Doppler spread due to higher $\zeta^{(1)}$ in the case of fast-fading. A comparison between flat fading and a three tap channel model in the absence of phase noise shows a loss as large as 23 dB due to the well-known intrinsic interference problem in SMT systems [9].

In Fig. 7, we show the sensitivity of SMT in terms of SER using hard-decisions. The zero-th order Taylor series approximate of (23) is also plotted and seem to fit well with the numerical trials for all constellations. It is clear that higher constellations suffer more from phase noise impact while SMT and DMT have equivalent SER performance.

V. CONCLUSIONS

We have studied the influence of oscillator phase noise and small-scale channel fading on SMT system performance. The ICI and ISI components, that caused time and frequency nuances, were analyzed in detail providing insight into the sensitivity of SMT modulation. By analytical derivations and simulation validation, we have shown that self-interference due to phase noise has no influence on SMT systems, while at the same time it suffers from significant ISI. We provided the analysis of the effects of resulting interference separately under various channel conditions. The performance comparison of SMT and DMT was also discussed to outline the effect of SMT's frequency confinement on ICI performance and its superiority in certain scenarios.

REFERENCES

- [1] C. Lele, P. Siohan, and R. Legouable, "2 dB better than CP-OFDM with OFDM/OQAM for preamble-based channel estimation," in *IEEE International Conference on Communications (ICC)*, May 2008.
- [2] G. Cherubini and et al., "Filter bank modulation techniques for very high speed digital subscriber lines," *Communications Magazine, IEEE*, vol. 38, no. 5, pp. 98–104, May 2000.
- [3] N. Benvenuto, G. Cherubini, and L. Tomba, "Achievable bit rates of DMT and FMT systems in the presence of phase noise and multipath," in *51st IEEE Vehicular Technology Conference Proceedings (VTC)*, vol. 3, 2000, pp. 2108–2112 vol.3.
- [4] N. Moret and A. Tonello, "Performance of filter bank modulation with phase noise," *Wireless Communications, IEEE Transactions on*, vol. 10, no. 10, pp. 3121–3126, October 2011.
- [5] A. Assalini, S. Pupolin, and A. Tonello, "Analysis of the effects of phase noise in filtered multitone (FMT) modulated systems," in *Global Telecommunications Conference, 2004. GLOBECOM '04. IEEE*, vol. 6, Nov 2004, pp. 3541–3545 Vol.6.
- [6] N. Moret and A. Tonello, "Filter bank transmission systems: Analysis with phase noise," in *Wireless Communication Systems, 2009. ISWCS 2009. 6th International Symposium on*, Sept 2009, pp. 498–501.
- [7] A. Armada, "Understanding the effects of phase noise in orthogonal frequency division multiplexing (OFDM)," *Broadcasting, IEEE Transactions on*, vol. 47, no. 2, pp. 153–159, Jun 2001.
- [8] G. Lin, N. Holte, and L. Lundheim, "Design of robust pulses to carrier frequency offset for OFDM/OQAM system," in *IEEE Global Telecommunications Conference, (GLOBECOM)*, vol. 3, Nov 2005.
- [9] T. Ihalainen, A. Ikhlef, J. Louveaux, and M. Renfors, "Channel equalization for multi-antenna FBMC/OQAM receivers," *Vehicular Technology, IEEE Transactions on*, vol. 60, no. 5, pp. 2070–2085, Jun 2011.
- [10] P. Siohan, C. Siclet, and N. Lacaille, "Analysis and design of OFDM/OQAM systems based on filterbank theory," *IEEE Trans. Signal Process.*, vol. 50, no. 5, pp. 1170–1183, May 2002.
- [11] M. Bellanger, *Digital Processing of Signals: Theory and Practice*. New York, USA: Wiley, 1989.
- [12] J. G. Proakis and M. Salehi, *Communication Systems Engineering*, 2nd ed. Upper Saddle River, NJ, USA: Prentice-Hall, Aug. 2001.
- [13] Y.-C. Liao and K.-C. Chen, "Estimation of stationary phase noise by the autocorrelation of the ICI weighting function in OFDM systems," *Wireless Communications, IEEE Transactions on*, vol. 5, no. 12, pp. 3370–3374, December 2006.